DNA replication and spindle checkpoints cooperate during S phase to delay mitosis and preserve genome integrity

Maria M. Magiera, Elisabeth Gueydon, and Etienne Schwob

Institute of Molecular Genetics, Centre National de la Recherche Scientifique Unité Mixte de Recherche 5535 and University of Montpellier, 34293 Montpellier, France

Deoxyribonucleic acid (DNA) replication and chromosome segregation must occur in ordered sequence to maintain genome integrity during cell proliferation. Checkpoint mechanisms delay mitosis when DNA is damaged or upon replication stress, but little is known on the coupling of S and M phases in unperturbed conditions. To address this issue, we postponed replication onset in budding yeast so that DNA synthesis is still underway when cells should enter mitosis. This delayed mitotic entry and progression by transient activation of the S phase, G2/M, and spindle assembly checkpoints. Disabling both Mec1/ATR- and Mad2-dependent controls caused lethality in cells with deferred S phase, accompanied by Rad52 foci and chromosome missegregation. Thus, in contrast to acute replication stress that triggers a sustained Mec1/ATR response, multiple pathways cooperate to restrain mitosis transiently when replication forks progress unhindered. We suggest that these surveillance mechanisms arose when both S and M phases were coincidently set into motion by a unique ancestral cyclin–Cdk1 complex.

Introduction

Maintenance of genome integrity depends on the successful completion of several cellular events, the most prominent being genome duplication during S phase and chromosome segregation in mitosis. These key cell cycle events are orchestrated in all eukaryotes by waves of Cdk activity. In yeast, three G1 cyclins (Cln1–3), two B-type cyclins (Clb5,6), and four mitotic cyclins (Clb1–4) associate with a single catalytic subunit (Cdc28/Cdk1) to promote start, S phase, and mitosis, respectively (Nasmyth, 1996). Interestingly, a single monomolecular Cdk module suffices for fission yeast proliferation, raising the question of how the order between S phase and mitosis is maintained (Coudreuse and Nurse, 2010). Exogenous stress or cell cycle defects trigger cellular surveillance mechanisms (checkpoints), which delay cell cycle progression until the problem is resolved (Weinert and Hartwell, 1988). Mechanisms governing cell cycle progression and monitoring its accuracy are often defective in cancer and have therefore been studied extensively (Bartek and Lukas, 2007; Malumbres and Barbacid, 2009).

Chromosome replication is set up in late M-G1 by formation of prereplication complexes made of Orc1–6, Cdc6, Cdt1, and Mcm2–7 proteins on future sites of bidirectional DNA synthesis called origins (Raghuraman et al., 2001; McGuffee et al., 2013). At G1/S, S-phase Cdk (Clb5,6–Cdk1) and Dbf4-dependent kinase (DDK; Dbf4–Cdc7) become active and phosphorylate several proteins required or DNA replication initiation (Labib, 2010; Tanaka and Araki, 2010). DNA synthesis starts at a subset of these origins and continues throughout S phase according to a spatiotemporal replication program that is influenced by chromatin context, subnuclear localization, the availability of limiting initiation factors, and checkpoint controls (Raghuraman et al., 2001; Zegerman and Diffley, 2010; Aparicio, 2013). Completion of DNA replication is key to genome integrity, as incompletely replicated chromosomes fail to segregate correctly and may break during mitosis. However, because origin firing is partly stochastic, the time of replication completion cannot be

The Rockefeller University Press $30.00
J. Cell Biol. Vol. 204 No. 2   165–175
www.jcb.org/cgi/doi/10.1083/jcb.201306023

JCB   165

THE JOURNAL OF CELL BIOLOGY

predetermined (Hyrien and Goldar, 2010; Rhind et al., 2010). Hence, it has been assumed that checkpoints monitor either the presence of unreplicated DNA or DNA synthesis itself and delay mitosis until all chromosomes are fully copied (Hartwell and Weinert, 1989; Li and Deshaies, 1993). Yet, cells that fail to initiate DNA replication nevertheless enter mitosis with little or no delay, indicating that unreplicated DNA does not prevent mitosis (Kelly et al., 1993; Piatti et al., 1995).

The dependence of mitosis upon completion of DNA replication has been studied mostly using drugs or mutations that interfere with replication fork progression. This identified an evolutionarily conserved pathway (Mec1, Ddc2, Chk1, and Rad53 in budding yeast; ATR, ATRIP, Chk1, and Chk2 in mammals), which is essential for fork stability and cell viability when DNA replication is perturbed. Cell cycle arrest under these conditions is caused by accumulation of abnormal DNA structures and excess primed single-strand DNA (Labib et al., 2001; Zou and Elledge, 2003; Shiotani and Zou, 2009; Van et al., 2010). However, it remains unclear whether this pathway senses normally progressing forks. The ATR–Chk1–Cdc25A pathway is activated during unperturbed S phase in cancer cell lines (Sørensen et al., 2004; Petermann et al., 2006) and during embryogenesis in mice but not in adult tissues (Murga et al., 2009). Thus, replication stress and checkpoint activation might be constitutive in rapidly proliferating cells but not in finely tuned somatic cells. Evidence from yeast also suggests that cells having an extended S phase can enter mitosis with hyporeplicated DNA without being detected by checkpoints (Lengronne and Schwob, 2002; Torres-Rosell et al., 2007; Dulev et al., 2009). Hence, whether or not an unperturbed S phase elicits a checkpoint capable of restraining mitotic entry remains an open question. Because chromosome replication is normally completed before mitosis begins (Schwob et al., 1994), this question could not be addressed satisfactorily without perturbing S phase. To create a situation in which chromosomes are still replicating at the time of normal mitosis, we postponed S-phase onset without affecting its duration and tested whether this delayed S phase was able, or not, to restrain mitosis.

Results and discussion

Delaying S-phase onset delays mitotic entry

Yeast cells were engineered so to activate their S-phase inducers S-phase Cdk and DDK later in the cell cycle. Deleting *CLB5* and *6* delays S-phase onset by 30 min compared with wild type, until activation of the next Cdk complex (Clb3,4–Cdk1) compensates for the lack of Clb5,6 (Schwob et al., 1994; Hu and Aparicio, 2005). Once started, S phase took the same time as in wild type (Fig. 1 A). To avoid caveats from cyclin deregulation, we also postponed S phase by expressing *DBF4*, coding the regulatory subunit of DDK, from the G2-specific *SWI5* promoter; this caused a similar 25–30-min delay without affecting S duration (Fig. 1 A). Strikingly, anaphase determined by the splitting of tetracycline repressor (TetR)-GFP marked sister chromatids (Michaelis et al., 1997) culminated at 90–100 min in *clb5,6* and *SWI5pr-DBF4* cells, instead of 70–80 min in wild type (Fig. 1 B).

Plotting anaphase onset relative to budding normalizes for variability in α-factor release kinetics between different strains and experiments (Fig. 1 B). Using this measure, we found that anaphase was delayed on average 17 and 12 min in *clb5,6* and *SWI5pr-DBF4* cells, respectively (Fig. 1 C). To rule out that this delay might stem from defects in previous cycles, we expressed *CLB5* conditionally from the tight *GALS* promoter (Mumberg et al., 1994) and turned it off before α-factor release, which gave identical results (Fig. S1 A). Thus, delaying S-phase onset by ∼30 min using independent strategies caused a ∼15-min delay in anaphase but no failure in mitosis or cytokinesis. *clb5,6* and *SWI5pr-DBF4* cells are enlarged (see Fig. 3 D) but show little genome instability (Lengronne and Schwob, 2002), suggesting that ongoing DNA synthesis triggers a checkpoint restraining mitosis until S phase is completed, after which cells proceed normally through mitosis.

An explanation for this anaphase delay could be that *clb5,6* and *SWI5pr-DBF4* cells suffer replication stress, as after deoxynucleotide triphosphate shortage or DNA damage, which slow S phase. To monitor S-phase kinetics more precisely than by FACS, we designed a novel assay based on brief ethynyl-deoxyuridine (EdU) pulses in synchronized cells to visualize ongoing DNA replication by microscopy (Fig. 1 D). This enabled detection of S-phase onset and termination and showed that once started, DNA replication proceeded very similarly in wild-type and *GALS-CLB5 clb6* cells (Fig. 1, E and F), corroborating a previous study (Donaldson et al., 1998). High-resolution SDS-PAGE and Phos-tag gels also failed to detect Rad53 hyperphosphorylation during S phase in *GALS-CLB5 clb6* cells, indicating an absence of replication stress (Fig. S1 B; Tercero et al., 2003). Finally, the viability of *GALS-CLB5 clb6* and *SWI5pr-DBF4* cells did not depend on *MEC1*, *RAD53*, or *CHK1*, in contrast to cells experiencing replication stress (Fig. S1 C). Together, this demonstrates that *clb5,6* and *SWI5pr-DBF4* cells have a replication fingerprint similar to wild-type cells and do not overtly activate the DNA damage response (DDR). Thus, although taking place later in the cell cycle, DNA replication in *clb5,6* and *SWI5pr-DBF4* cells has all the attributes of a physiological S phase. We conclude that unperturbed DNA replication can delay chromosome segregation.

Ongoing DNA replication delays both G2/M and anaphase onset

To investigate how DNA replication delays mitosis, we first monitored M-phase Cdk activation. Clb2–Cdk1 activity measured in vitro or in vivo (Foiani et al., 1995; Liu and Wang, 2006) was delayed 15–20 min in *clb5,6* cells compared with wild type (Figs. 2 A and S2 A). Because Clb2 and Clb3 accumulate normally (Fig. S2 B), we suspected that Cdc28/Cdk1 was inhibited by Swe1-dependent phosphorylation on Tyr19. Since *SWE1* deletion advances S phase and thus mitosis in *clb5,6* cells (Hu and Aparicio, 2005), we scored anaphase in *SWI5pr-DBF4 swe1* and *SWI5pr-DBF4 cdc28-F19* cells and found that part of the delay was suppressed (Fig. 2, B and C). Thus, Swe1-dependent Cdk1 inhibition is partly responsible for the mitotic delay triggered by ongoing DNA replication, consistent with Swe1 accumulation and Cdc28^{Tyr19} phosphorylation during unperturbed S phase
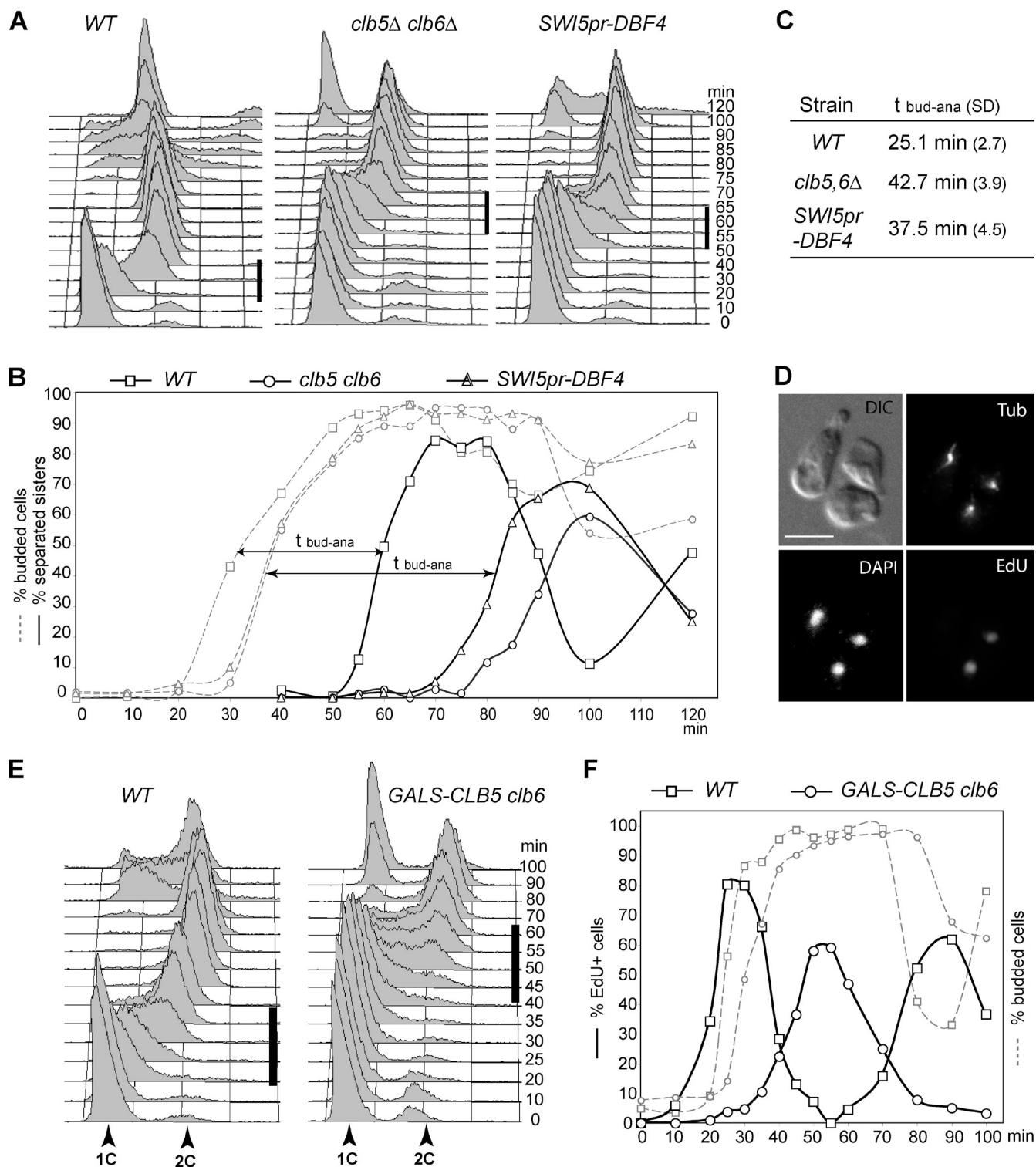
Figure 1. **Anaphase is delayed when DNA replication is delayed.** (A) DNA content after α-factor release in wild-type (WT; E1149), *clb5 clb6* (E1812), and *SWI5pr-DBF4* (E2011) cells. Black bars, S phase. (B) Sister chromatid separation (two TetR-GFP dots) in the strains above. Arrows, anaphase onset relative to budding. Representative data from three repeats. (C) $t_{bud-ana}$ calculated from three experiments. (D) Detection of ongoing DNA replication by EdU pulse labeling. TK-hENT1 yeast cells (E3087) were pulsed for 5 min with EdU, fixed, and processed for tubulin (Tub), DAPI, and EdU detection. DIC, differential interference contrast. Bar, 5 µm. (E) DNA content of wild-type (E3087) and *GALS-CLB5 clb6* cells after α-factor release in SC dextrose medium at 30°C. (F) Ongoing DNA replication in wild-type (E3087) and *GALS-CLB5 clb6* (E4495) cells labeled for 5 min with EdU; representative data from two repeats ($n > 100$).
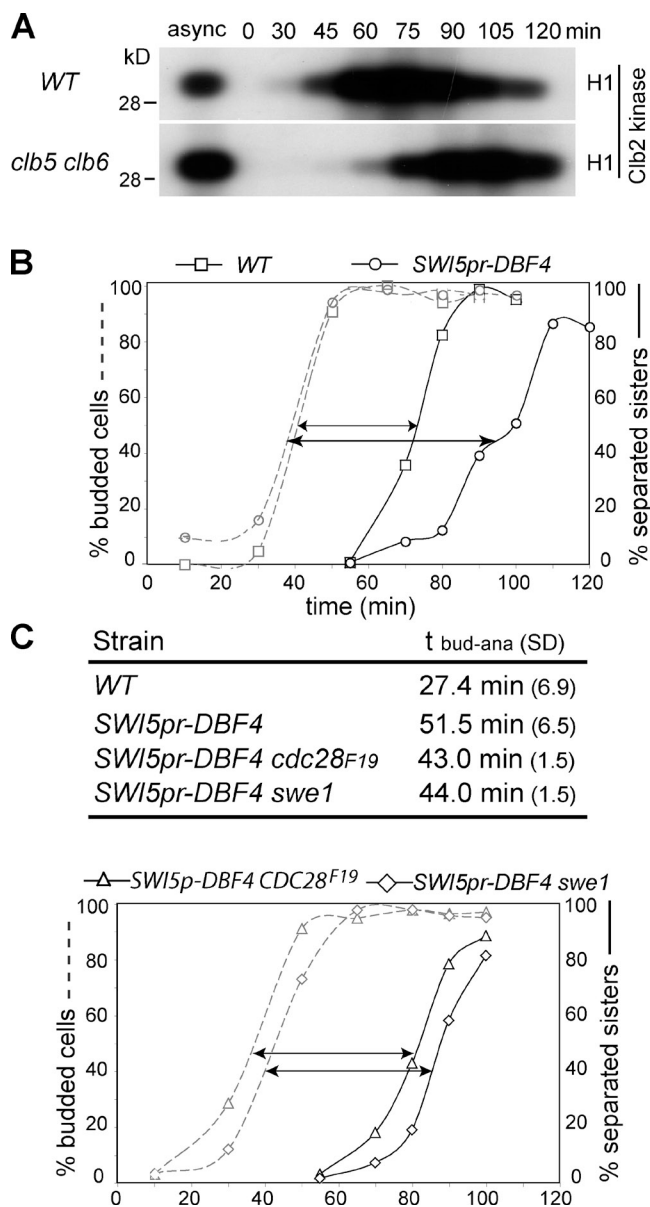
Figure 2. **Role of Cdc28^{Y19} in the replication-induced anaphase delay.** (A) In vitro Clb2-associated H1 kinase activity after α-factor release in wild-type (WT; E001) and *clb5 clb6* (E145) cells. async, asynchronous. (B) Anaphase onset in wild-type (E1149), *SWI5pr-DBF4* (E2011), *SWI5pr-DBF4 swe1* (E2711), and *SWI5pr-DBF4 cdc28^{Y19F}* (E2704) cells after release from α-factor. Arrows indicate $t_{bud-ana}$ ($n > 100$). (C) Relative anaphase timing in the strains indicated above. Experiments were performed twice and scored independently by two individuals.

(Liu and Wang, 2006). Although Cdc28^{Tyr19} phosphorylation was initially ruled out as being responsible for the hydroxy-urea (HU)–induced arrest in budding yeast (Amon et al., 1992; Sorger and Murray, 1992), we suggest here that Cdc28^{Tyr19} inhibition plays an ancillary role in the coupling of S and M phases under physiological conditions.

The S-phase checkpoint contributes but is not essential for the viability of *clb5,6* cells

To identify other pathways responsible for the anaphase delay caused by DNA replication, we looked for synthetic lethality

between *GALS-CLB5 clb6* cells and DDR mutants. Deletion of *MEC1, RAD9* or introduction of the checkpoint-deficient *mrc1AQ* allele had no major effect on the viability of *GALS-CLB5 clb6* cells grown on glucose, in which S phase is delayed (Fig. 3 A). A genome-wide synthetic genetic array screen also failed to reveal synthetic lethality with other DDR components (unpublished data), indicating that this pathway is either not involved in the replication-induced anaphase delay or that it contributes only partially. Indeed, we noticed that *GALS-CLB5 clb6 mec1* cells formed smaller colonies on glucose than galactose, suggesting that loss of Mec1 slowed cell division or caused lethality in a fraction of cells (Fig. 3 A). One explanation for the viability loss of *GALS-CLB5 clb6 mec1* cells could be that they attempt mitosis before DNA replication is completed. In fact, *GALS-CLB5 clb6 mec1* cells entered anaphase slightly earlier than *GALS-CLB5 clb6* cells (Fig. 3 B), indicating that the Mec1/ATR checkpoint helps to delay anaphase when DNA replication is ongoing but is not solely responsible for it.
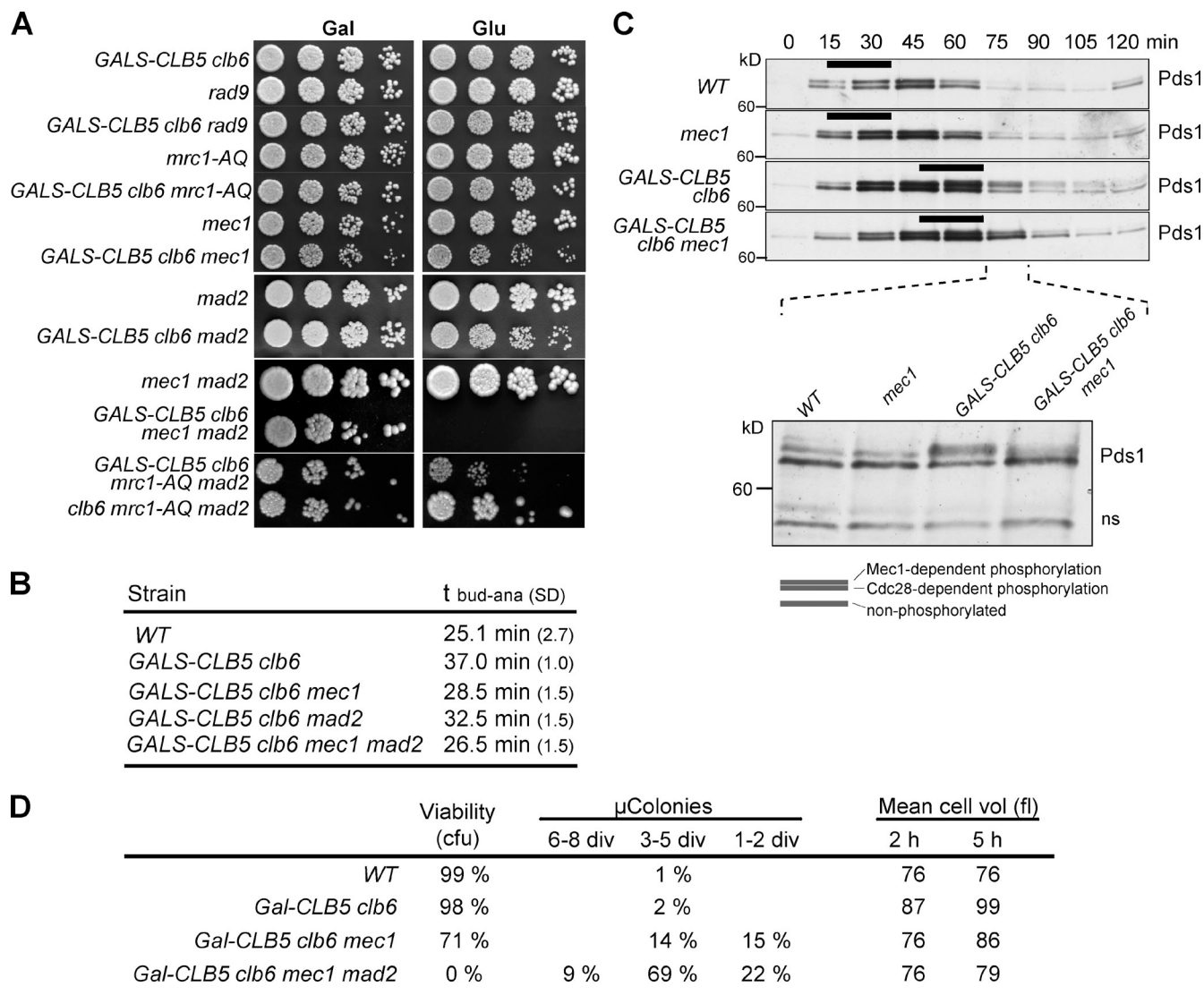
Securin is stabilized by Mec1-dependent and -independent mechanisms

As securin proteolysis is key for anaphase onset and a target of the Mec1–Chk1 pathway, we monitored Pds1 phosphorylation and proteolysis in *GALS-CLB5 clb6* cells, in the presence or absence of *MEC1*. Pds1 runs as a doublet on SDS-PAGE during S and G2 and is degraded in an anaphase-promoting complex (APC)^{Cdc20}–dependent manner at the meta- to anaphase transition (Cohen-Fix et al., 1996; Agarwal and Cohen-Fix, 2002). We noticed that the upper band was broader in *GALS-CLB5 clb6* cells (suggestive of hyperphosphorylation), and Pds1 was degraded ∼15 min later compared with wild type (Fig. 3 C). The slower migrating band likely corresponds to Pds1 stabilized by Chk1 phosphorylation (Cohen-Fix and Koshland, 1997) because it was lost when *MEC1* was deleted. However, this did not advance Pds1 degradation (Fig. 3 C). We conclude that (a) Mec1–Chk1 is induced during S phase in *GALS-CLB5 clb6* cells yet to a level insufficient to cause the Rad53 hyperphosphorylation seen in HU (Fig. S1 B), and (b) Mec1-dependent Pds1 phosphorylation is not solely responsible for its tardy degradation when replication is ongoing.

Mec1 and Mad2 pathways cooperate to delay mitosis when DNA replication is ongoing

Because Pds1 proteolysis was still delayed in *GALS-CLB5 clb6 mec1* cells, we suspected that the APC^{Cdc20} was not fully active. Mad2 is an inhibitor of APC^{Cdc20} and central player of the spindle assembly checkpoint (SAC). Deletion of *MAD2* in *GALS-CLB5 clb6* cells affected their proliferation similarly to *MEC1* deletion (Fig. 3 A) and slightly advanced their anaphase onset (Fig. 3 B). This raised the possibility that Mec1- and Mad2-dependent checkpoints independently delay mitosis when DNA replication is ongoing. If this were the case, disabling both checkpoints might be lethal for late-replicating cells. Strikingly, *GALS-CLB5 clb6 mec1 mad2* cells grew happily on galactose plates (normal replication) but produced no colonies on glucose

A

Gal | Glu

GALS-CLB5 clb6
rad9
GALS-CLB5 clb6 rad9
mrc1-AQ
GALS-CLB5 clb6 mrc1-AQ
mec1
GALS-CLB5 clb6 mec1

mad2
GALS-CLB5 clb6 mad2

mec1 mad2
GALS-CLB5 clb6 mec1 mad2
GALS-CLB5 clb6 mrc1-AQ mad2
clb6 mrc1-AQ mad2

B

Strain	$t_{bud-ana}$ (SD)
WT	25.1 min (2.7)
GALS-CLB5 clb6	37.0 min (1.0)
GALS-CLB5 clb6 mec1	28.5 min (1.5)
GALS-CLB5 clb6 mad2	32.5 min (1.5)
GALS-CLB5 clb6 mec1 mad2	26.5 min (1.5)

C

D

	Viability (cfu)	µColonies			Mean cell vol (fl)	
		6-8 div	3-5 div	1-2 div	2 h	5 h
WT	99 %		1 %		76	76
Gal-CLB5 clb6	98 %		2 %		87	99
Gal-CLB5 clb6 mec1	71 %		14 %	15 %	76	86
Gal-CLB5 clb6 mec1 mad2	0 %	9 %	69 %	22 %	76	79

Figure 3. **Deletion of *MEC1* and *MAD2* is lethal when S phase is delayed.** (A) Strains of the indicated genotypes were spotted at serial fivefold dilutions on YEP plates containing either galactose (Gal) or glucose (Glu) to induce or repress Clb5 synthesis, respectively. (B) Anaphase onset relative to budding ($t_{bud-ana}$) was calculated as in Fig. 2 B; values are from two experiments and dual scoring. (C) Western blot of Pds1-myc18 in synchronized wild-type (E686), *mec1 sml1* (E2911), *GALS-CLB5 clb6* (E2909), and *GALS-CLB5 clb6 mec1* (E2908) cells. Bars indicate S phase measured by FACS (Fig. S2 C). (bottom) Reloading of the 75-min point; ns, nonspecific band for loading control. Black lines indicate that intervening lanes have been spliced out. (D) Cells were grown in YEPRG, transferred to YEPD medium, or spotted on YPD plates. Microcolony formation was scored after 24 h (Fig. S3 B), and mean cell volume was measured 2 and 5 h after shift to YEPD. WT, wild type. div, divisions; cfu, colony-forming unit.

(delayed replication; Fig. 3 A). Thus, *MEC1* and *MAD2* are essential when S phase occurs late but dispensable if early. Because *mec1 mad2* double deletion advanced anaphase further than *mec1* alone (Fig. 3 B), we wondered whether *GALS-CLB5 clb6 mec1 mad2* cells died from checkpoint failure followed by mitotic catastrophe. Indeed most *GALS-CLB5 clb6 mec1 mad2* cells died rapidly after shift to glucose, with a cell volume smaller than the *GALS-CLB5 clb6* parent, consistent with escape from a transient checkpoint arrest (Fig. 3 D). The requirement of *MEC1* and *MAD2* for the viability of late-replicating cells was confirmed in *SWI5pr-DBF4* cells, in which genetic analysis revealed a fourfold lower than expected frequency of *SWI5pr-DBF4 mec1 mad2* progeny (unpublished data). We conclude that late-replicating cells rely on both the S-phase checkpoint and the SAC for viability.

The SAC is transiently activated during S phase

Because it was not anticipated, we explored further the role of Mad2 and SAC in preventing mitosis while DNA replication is ongoing. *MAD1* deletion or expression of the dominant *CDC20-107* allele was also lethal in *GALS-CLB5 clb6 mec1* cells (Fig. 4 A), indicating that Mad2 keeps *GALS-CLB5 clb6 mec1* cells alive by inhibiting APC^{Cdc20}. Mad2 binds monooriented kinetochores, and a single unattached kinetochore is sufficient to delay mitosis through the SAC (Li and Nicklas, 1995; Chen et al., 1996; Gillett et al., 2004). Of note, kinetochores detach temporarily from microtubules upon centromere (CEN) replication, consistent with the early and transient SAC activation seen in unperturbed cell cycles (Brady and Hardwick, 2000; Kitamura et al., 2007). At around the same time, a small
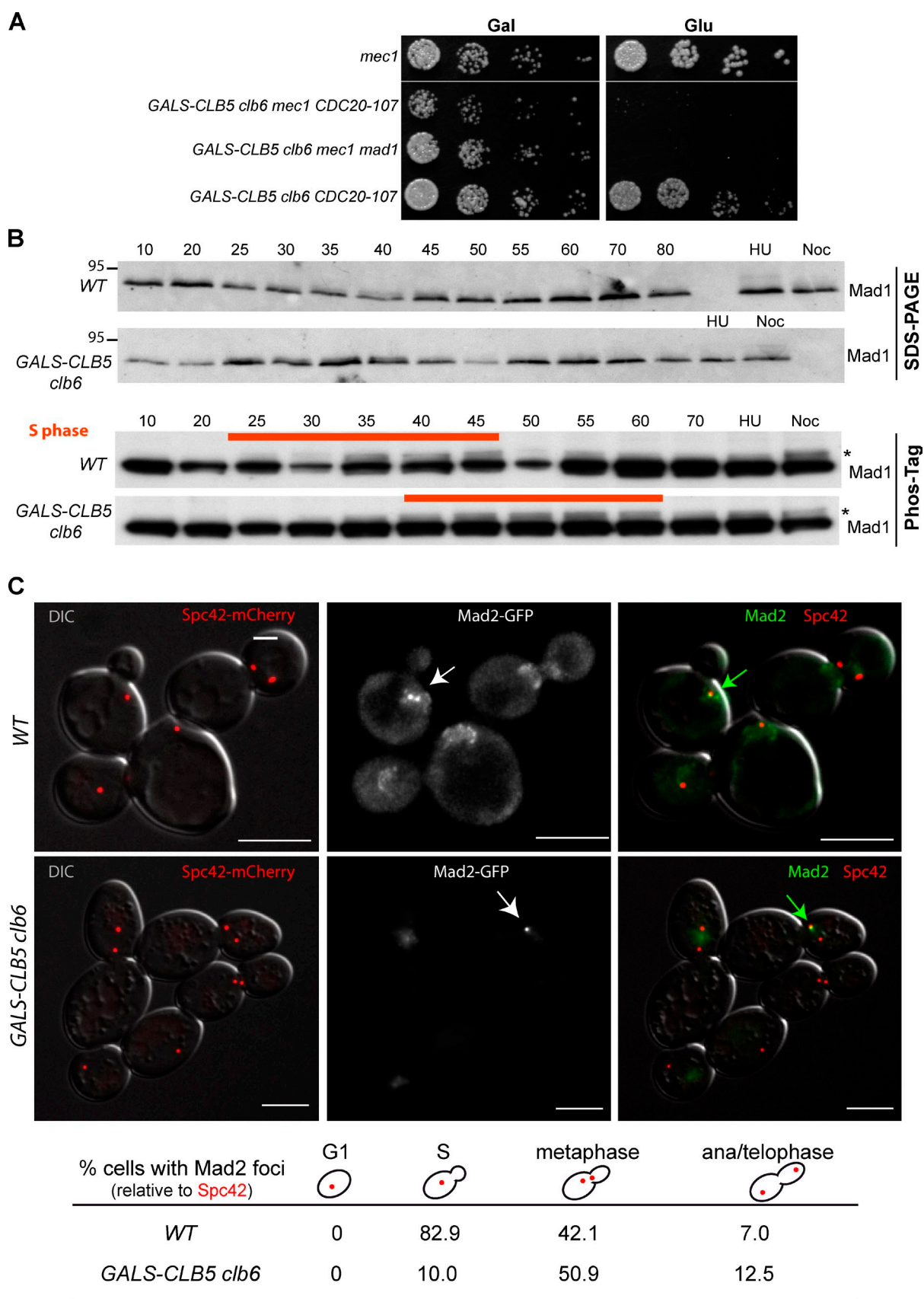
A

Gal   Glu

mec1

GALS-CLB5 clb6 mec1 CDC20-107

GALS-CLB5 clb6 mec1 mad1

GALS-CLB5 clb6 CDC20-107

B

10 20 25 30 35 40 45 50 55 60 70 80   HU Noc

95 —   *WT*   Mad1 / SDS-PAGE

95 —   *GALS-CLB5 clb6*   HU Noc   Mad1 / SDS-PAGE

S phase   10 20 25 30 35 40 45 50 55 60 70 HU Noc

WT   * Mad1 / Phos-Tag

GALS-CLB5 clb6   * Mad1 / Phos-Tag

C

DIC   Spc42-mCherry   Mad2-GFP   Mad2 Spc42   *WT*

DIC   Spc42-mCherry   Mad2-GFP   Mad2 Spc42   *GALS-CLB5 clb6*

% cells with Mad2 foci (relative to Spc42)	G1	S	metaphase	ana/telophase
WT	0	82.9	42.1	7.0
GALS-CLB5 clb6	0	10.0	50.9	12.5

Figure 4. **The SAC is transiently activated during S phase.** (A) Viability of *GALS-CLB5 clb6 mec1* cells depends on the SAC. Gal, galactose; Glu, glucose. (B) Mad1 phosphorylation during S phase. Wild-type (WT; E3087) and *GALS-CLB5 clb6* (E4495) cells released from G1 were incubated in YEPD 30°C for the indicated times (in minutes) or 90 min in the presence of 0.2 M HU or 15 µg/ml nocodazole. Cell extracts (10 µg) were resolved on SDS-PAGE (top)

fraction of Mad1 gets phosphorylated (Hardwick and Murray, 1995). To see whether this was linked to DNA replication, we followed Mad1 phosphorylation using Phos-tag gels (Kinoshita et al., 2006). A fraction of Mad1 shifted 25–45 min after release in wild type, but this occurred later (40–60 min) in *GALS-CLB5 clb6* cells, matching their different replication time (Fig. 4 B). This S-phase Mad1 phosphorylation is not caused by spindle assembly stress as initially suggested (Chen et al., 1996), as bipolar spindles form at the same time in wild-type and *clb5,6* cells (Fig. S3 A), yet Mad1 phosphorylation is delayed in the latter. Rather, we propose that the SAC is activated upon kinetochore disassembly when CENs are duplicated and that this occurs later when S phase is delayed. Consisten with this idea, using deconvolution microscopy, we were able to detect Mad2-GFP foci proximal to centrosomes (spindle pole bodies [SPBs]) in small budded wild-type cells in S phase but rarely in anaphase and never in unbudded G1 cells. In contrast, Mad2-GFP foci were seen mostly in large budded *GALS-CLB5 clb6* cells having already separated their SPBs (Fig. 4 C). These results confirm that spindle formation is uncoupled from DNA replication in budding yeast and strongly suggest that CEN replication transiently activates the SAC. We propose that delayed CEN duplication prevents anaphase entry through kinetochore detachment causing SAC activation.

DNA damage and chromosome loss in *GALS-CLB5 clb6* cells lacking Mec1 and Mad2

Analysis of *GALS-CLB5 clb6 mec1 mad2* cells showed that they entered anaphase with little or no delay, and also exited mitosis faster than *GALS-CLB5 clb6* cells. To see whether this precipitous mitosis causes DNA damage or double-strand breaks, we scored Rad52 recombination foci. 150 min after *CLB5* shutoff, 30% of *GALS-CLB5 clb6 mec1 mad2* cells contained single or multiple nuclear Rad52 foci compared with 3% in wild type (Fig. 5 A). When released from G1, wild-type cells showed Rad52 foci during two successive S phases (45 and 120 min; Fig. 5 B), as expected (Lisby et al., 2001). This wave of Rad52-positive cells was delayed in *GALS-CLB5 clb6* cells, consistent with their delayed S phase. Deletion of *MEC1* increased Rad52 foci in wild-type and *GALS-CLB5 clb6* cells, reflecting Mec1's requirement for fork stability during S phase. However, the fraction of Rad52 foci increased further in *GALS-CLB5 clb6 mec1* cells, from 120 min onwards (Fig. 5 B). Deleting *MAD2* did not increase further Rad52 foci, despite having a strong effect on the viability of *GALS-CLB5 clb6 mec1* cells. This could be explained if Mad2 loss caused death of *clb5 clb6 mec1 sml1* cells mostly by chromosome missegregation rather than by increasing DNA damage.

Therefore, we scored the number and position of GFP-marked *URA3* loci relative to nuclear morphology. Wild-type cells showed the expected patterns of *tetO*/TetR-GFP signals: a single dot from G1 to metaphase and then splitting of the dots in early anaphase followed by segregation of the dots to opposite poles in telophase. We defined four classes of abnormal patterns, as shown in Fig. 5 C. *GALS-CLB5 clb6* cells contained more single dots within an elongating nucleus (nondisjunction), as expected if anaphase is delayed until replication is completed. *GALS-CLB5 clb6 mec1* cells showed patterns that may correspond to cohesion defects or rearrangements of the *tetO* array. *MAD2* deletion mainly caused chromosome missegregation with 1:0 or 2:0 patterns. Lastly, deletion of both *MEC1* and *MAD2* mostly increased chromosome loss events in late-replicating cells (Fig. 5 C). The high rate of chromosome V loss in *GALS-CLB5 clb6 mec1 mad2* cells, extrapolated to the number of yeast chromosomes, most likely accounts for the stark lethality of these cells. Our observations are corroborated by a recent study that detected, using a genome-wide approach, a decreased fitness of *clb5 clb6* cells with cohesion and SAC signaling mutants (Haber et al., 2013).

Mec1 and Mad2 checkpoints are active at a low level during DNA replication

The fact that Mec1 and Mad2 each contribute to the viability and anaphase delay implies that these checkpoints are active in *clb5,6* cells. However, Rad53 is not hyperphosphorylated during S phase in these cells, despite their checkpoint proficiency (Fig. S1 B). Using Phos-tag gels, we found that Rad53 in fact exists as three phosphoisoforms in unperturbed wild-type and *clb5 clb6* cells, with a shift toward the higher phosphoforms during S phase (Fig. S1 B, bottom). Thus, both our genetic and biochemical evidences indicate that the Mec1–Rad53 pathway is constitutively active at a low level during S, as suggested previously (Sørensen et al., 2004). Specific structures at normal or paused replication forks, such as single-strand DNA–replication protein A complexes, may generate a weak signal for Mec1–Rad53 activation (Cimprich and Cortez, 2008). Global signal strength would thus depend on the number of active forks and would dampen toward the end of S, releasing the brake for mitotic entry. Conversely, CEN replication would generate a transient but potent "wait anaphase" signal, delaying anaphase until sister kinetochores biorient.

Together, our data demonstrate that the replication checkpoint and SACs are active at a low level during S phase, sufficient to delay anaphase transiently. These signaling pathways, always active at a low surveillance mode during unperturbed cell cycles, can be amplified to emergency mode upon extrinsic stress, as witnessed by Rad53 hyperphosphorylation in HU (Fig. S1 B). Conversely, these anaphase-delaying signals may fall below threshold after all kinetochores have reassembled and when the number of active forks drops. This may explain why yeast mutants completing replication using fewer forks

or Phos-tag gels (bottom). Noc, nocodazole; asterisks, phosphorylated form. FACS is shown in Fig. 1 E. (C) Mad2 localization near SPBs during S phase. Wild-type (E3536) and *GALS-CLB5 clb6* (E3538) diploid cells heterozygous for *MAD2-GFP* and *SPC42-mCherry* were grown in SC at 30°C and imaged by deconvolution microscopy. Mad2 recruitment at kinetochores (arrows) Bars, 5 µm. Quantification indicates percentages of G1, S, metaphase, or anaphase cells in which Mad2 can be seen as a dot near SPBs. In the remaining cells, Mad2 shows diffuse nuclear staining. DIC, differential interference contrast.
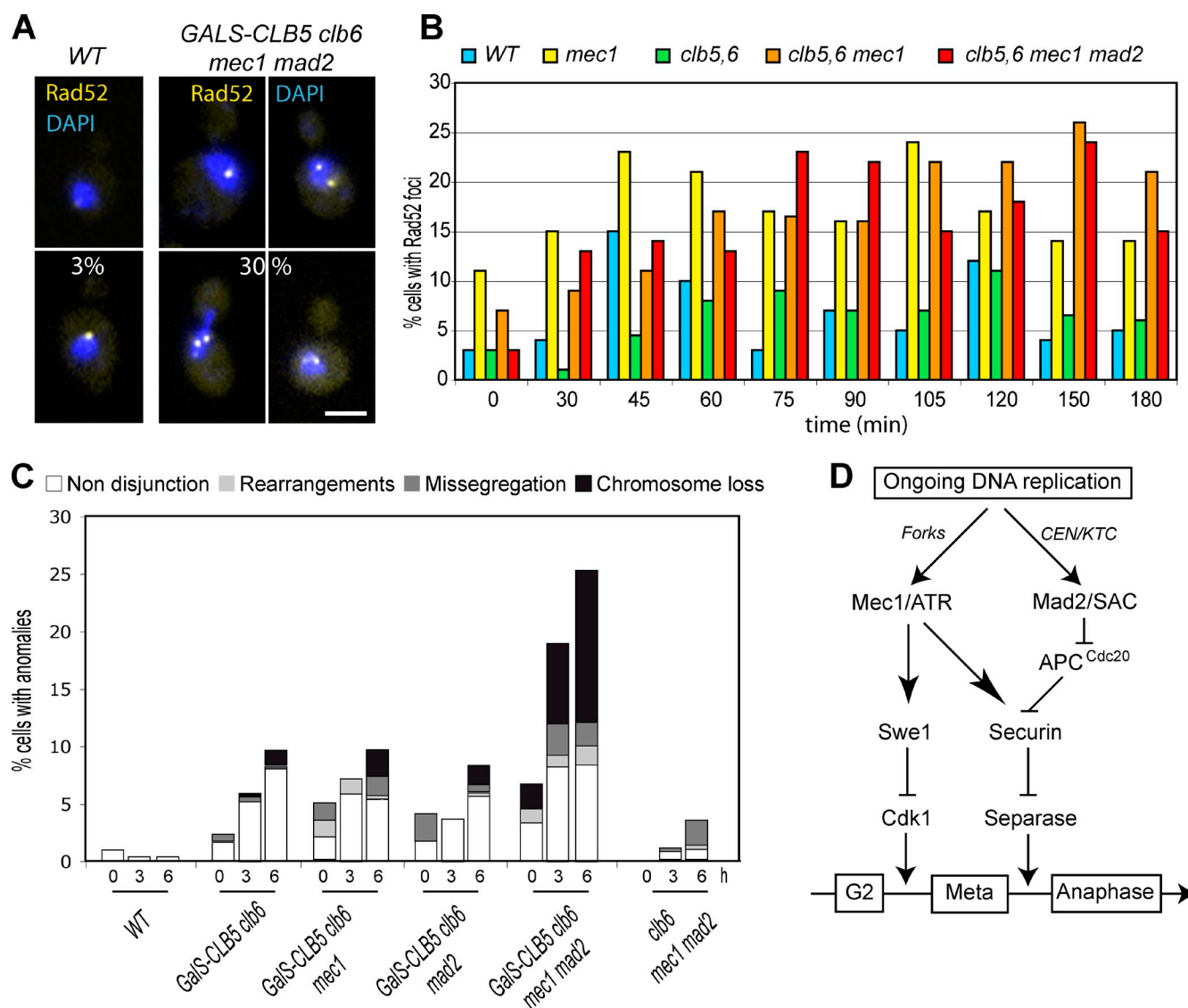
Figure 5. **Chromosome instability in late-replicating cells lacking Mec1 and Mad2.** (A) Representative images of asynchronous wild-type (WT; E1925) and *GALS-CLB5 clb6 mec1 mad2* (E2923) cells expressing Rad52-GFP, 150 min after shift to YEPD. The percentage of cells containing Rad52-GFP foci in each strain is indicated. Bar, 5 µm. (B) Rad52 foci–positive cells after α-factor release of wild-type (E2774), *GALS-CLB5 clb6* (E2178), *GALS-CLB5 clb6 mec1* (E2966), and *GALS-CLB5 clb6 mec1 mad2* (E2923) cells; n > 100. (C) Cells of the indicated genotypes (E2288, E2172, E3395, E3397, E3399, and E3396) were analyzed for abnormal chromosome segregation patterns as indicated in the Materials and methods; n > 100. (D) Model for the cooperation of Mec1/DDR and Mad2/SAC surveillance mechanisms in monitoring ongoing DNA replication and preventing precocious mitotic entry.

can enter anaphase with incompletely replicated chromosomes (Lengronne and Schwob, 2002; Torres-Rosell et al., 2007; Dulev et al., 2009). We propose the following scenario for the strong synthetic lethality of *clb5 clb6* and *mec1 mad2* mutants (Figs. 3 A and 4 A): in *clb5 clb6* cells, mitotic entry and anaphase are prevented until replication is completed by the joint action of Mec1- and Mad2-dependent pathways operating through signals emanating from ongoing forks and detached kinetochores, respectively (Fig. 5 D). Mec1 has several roles beyond signaling replication fork stress, but the contribution of the latter to the viability of *clb5 clb6 mad2* cells is supported by the viability loss conferred by the *mrc1-AQ* mutation (Fig. 3 A). Without Mec1, Mad2 signaling is sufficient to sustain viability, and vice versa. However, *clb5 clb6 mec1* cells suffer from increased double-strand break/Rad52 foci, perhaps as a

result of precocious spindle extension or mitosis, and *clb5 clb6 mad2* cells show increased chromosome missegregation (Feng et al., 2009; Haber et al., 2013). In the absence of both Mec1 and Mad2, ongoing replication is not signaled anymore, and *clb5 clb6* cells undergo anaphase before having finished DNA synthesis and before chromatid biorientation is reestablished. We suggest that this extreme case of synthetic lethality between Mec1/DDR and Mad2/SAC inhibition in late-replicating cells should be explored as a strategy to fight cancer cells that often show altered replication dynamics.

Checkpoints may have evolved to order S phase and mitosis in ancestral eukaryotes

Our results show that ongoing DNA synthesis inhibits mitosis using many of the mechanisms described after replication and

spindle stresses: Swe1-dependent Cdc28^{Y19} phosphorylation, Chk1-induced Pds1/securin stabilization, and Mad2-dependent APC^{Cdc20} inhibition. When during evolution did these checkpoints arise, and why do they subsist in organisms such as yeast in which they are dispensable for life? We suggest that the DDR and SAC evolved in ancestral eukaryotes, when both S phase and mitosis were set into motion by the same cyclinB–Cdk complex, and in which mechanisms delaying mitosis until replication is completed were essential to ensure the correct order of these events (Miranda-Saavedra et al., 2007). It has been shown that M-phase Cdk can also trigger S phase and that fission yeast living on a single monomolecular cyclin–Cdk module are highly dependent on the Wee1 regulatory loop (Moore et al., 2003; Coudreuse and Nurse, 2010). Checkpoint mechanisms probably became less important in modern eukaryotes because other mechanisms, i.e., the temporal separation and specialization of S-phase and M-phase cyclins, ensured that DNA replication is finished well before mitosis is attempted. However, their function remained essential to preserve genome integrity when cell cycle timing controls are overridden (as in this study), after replication stress or in rapid proliferation settings.

Materials and methods

Yeast strains and culture
The strains used in this study are listed in Table S1. These strains are congenic or backcrossed at least four times to W303 (*MATa ade2-1 trp1-1 can1-100 leu2-3,112 his3-11,15 ura3-1*). They were obtained by standard genetic techniques (Kaiser et al., 1994). The *GALS-CLB5* and *PDS1-18myc* strains were constructed using published protocols (Longtine et al., 1998; Janke et al., 2004). The *SWI5pr-DBF4* strain was made by integrating the Apa1-linearized plasmid D1361 at the *DBF4* locus. Plasmid D1361 contains 413 bp of the *SWI5* promoter fused to a truncated *DBF4* gene deleted for amino acids 333–702 in the YIplac204 vector (Gietz and Sugino, 1988). Integration generates a truncated *dbf4ΔC-ter* followed by a full-length *DBF4* driven by the G2/M-specific *SWI5* promoter. All strains that indicated *mec1* are also deleted for *SML1*. CLB2-PrA and CLB3-PrA constructs were provided by F. Cross (The Rockefeller University, New York, NY), *tetO336/ TetR-GFP* was provided by K. Nasmyth (Oxford University, Oxford, England, UK), *mrc1-AQ* was provided by P. Pasero (Institut de Génétique Humaine, Montpellier, France), *PDS1-myc18, mad1::LEU2, mad2::URA3, CDC20-107,* and *cdc28F19* were provided by S. Piatti (Centre de Recherche de Biochimie Macromoléculaire, Montpellier, France), *RAD52-GFP* was provided by R. Rothstein (Columbia University, New York, NY), *ADH-hENT1* was provided by K. Shirahige (University of Tokyo, Tokyo, Japan), *SPC29-CFP* was provided by B. Snydman (Yeast Resource Center, Seattle, WA), *MTW1-4GFP* and *CTF19-4GFP* were provided by T.U. Tanaka (University of Dundee, Dundee, Scotland, UK), and *SPC42-mCherry* was provided by Y. Watanabe (University of Tokyo, Tokyo, Japan). Unless stated otherwise, cells were grown in YEP (yeast extract peptone) medium containing 2% glucose (YPD [YEP dextrose]) or 1.8% raffinose and 0.2% galactose (YPRG). Cell concentration and volume were measured using the cell counter (CASY1 TTC; Schärfe System).

α-Factor release experiments
Cells were grown in YPD to 4×10^6 cell/ml, and 1 µg/ml α-factor was added twice (0 and 75 min) and left for 135 min until release by filtration or addition of 50 µg/ml pronase (EMD Millipore). Strains containing *GALS-CLB5* were grown in YPRG and shifted to YPD 60 min before release from α-factor.

EdU pulse labeling and detection
GPD-TK ADH-hENT1 cells (E3087) were grown in synthetic complete (SC) medium, synchronized with α-factor, and released in SC medium. Aliquots were pulsed with 10 µM EdU for 5 min in the same medium, immediately fixed in 2% PFA, and then permeabilized with 70% EtOH. Cells were incubated in PBS–1% BSA, washed in PBS, resuspended in 50 µl of Click-iT reaction mix containing 2 mM CuSO$_4$, 20 µM DY-530 azide (Dyomics), and

10 mM ascorbic acid in PBS, and left for 30 min in the dark. Cells were washed twice with PBS, incubated 30 min with 0.5 µg/ml DAPI, washed with PBS, and imaged.

Microscopy
For Rad52-GFP, Mtw1-GFP, and *tetO*/TetR-GFP detection, cells were grown in SC medium, centrifuged, resuspended in 10 µl of medium, and fixed by the addition of 1 ml of 80% ethanol (−20°C). For microscopy, 100 µl of cell suspension was added to 1 ml PBS, briefly sonicated, and concentrated to the desired density. 1.5 µl of cell suspension was put on a microscope slide and observed using the 100× Plan Apochromat, 1.4 NA objective on a microscope (DM6000; Leica). Images were acquired with a camera (CoolSNAP HQ²; Photometrics/Roper Scientific) and MetaMorph 7.6 (Molecular Devices) and then analyzed with ImageJ (National Institutes of Health). Experiments were performed at least twice, and samples were number coded and analyzed independently by two people. At least 100 cells were counted for each time point. The time interval between budding and anaphase ($t_{bud-ana}$) was calculated from times at half-maximal budding and sister chromatid splitting, respectively. Means and SD are indicated. Because *tetO* repeats are unstable in *mec1* strains, we monitored in Fig. 3 B the segregation of Mtw1-4GFP–marked kinetochores, which cluster as two close dots (∼0.8 µm apart) in metaphase and then separate by >4 µm in anaphase (Joglekar et al., 2009). For Mad2-GFP localization, diploids containing one *MAD2* and one *MAD2-GFP* allele were grown in SC dextrose medium at 30°C and immediately imaged using a 63× HCX Plan Apochromat, 1.4 NA objective, 13 z stacks of 0.3 µm, GFP and Cy3 filter cubes, 300-ms acquisition time, and no binning. The resulting dual-color images were deconvolved using Huygens Pro (Scientific Volume Imaging) with the following settings: volume processing, full restoration, supernatant ratio of 50, background offset of 100%, 20 iterations, quality change threshold of 0, and output format of 16-bit TIFF. Maximal projections of deconvolved images were generated with ImageJ and overlaid with the differential interference contrast image. For chromosome missegregation analysis (Fig. 5 C), cells were grown in YEP medium containing 2% raffinose and 0.1% galactose, shifted to YPD for 0, 3, or 6 h, stained with DAPI, and analyzed for abnormal chromosome segregation patterns according to the following classes: nondisjunction (one dot in extended nucleus), rearrangements (more than two dots in an extended nucleus), missegregation (two dots in same nuclear mass), and chromosome loss (nucleated cell without the CEN V dot).

Clb2-associated H1 kinase assay
In brief, ∼10^8 cells were washed twice in ice-cold stop mix buffer (150 mM NaCl, 1 mM NaN$_3$, 10 mM EDTA, and 50 mM NaF), resuspended in 90 µl kinase breakage buffer (KBB; 50 mM Tris-HCl, pH 7.5, 150 mM NaCl, 15 mM MgCl$_2$, and 1% NP-40 supplemented with proteases and phosphatases inhibitors), and broken 5×30 s with zirconium beads on a Vibrax at 4°C. Extracts were clarified for 7 min at 12,000 rpm at 4°C, and protein concentration was measured using a Bradford assay. Clb2 was immunoprecipitated at 4°C from 100 µg of extract using affinity-purified anti-Clb2 polyclonal antibodies diluted 1:600 and 15 µl of a 50% protein A–Dynabeads slurry preincubated in KBB + 1 mg/ml BSA. Immune complexes were diluted in 0.5 ml KBB and washed twice with KBB and thrice with 25 mM MOPS, pH 7.2, using a magnetic stand. For the kinase assay, beads were incubated 5 min in 6 µl histone buffer II (25 mM MOPS, pH 7.5, 15 mM MgCl$_2$, and 5 mM EGTA plus inhibitors) and then 15 min at 25°C after adding 10 µl kinase buffer (1 mg/ml H1, 25 mM MOPS, pH 7.2, 100 µM ATP, and 1 µCi γ-[^{32}P]ATP [3,000 Ci/mmol]).

Whole-cell protein extract from yeast cells
8–20 ml of yeast culture was centrifuged and resuspended in 1 ml of 10% TCA. Cells were concentrated to 200 µl in 10% TCA, and 200 µl of glass beads (Zirconia/Silica Beads; BioSpec Products, Inc.) was added. Cells were then lysed using a FastPrep 120 (Thermo Savant; MP Biomedicals). Supernatant was transferred to a new tube, the beads were washed twice with 200 µl of 10% TCA, and extracts were pooled. Extracts were centrifuged at 3,000 rpm for 10 min, and the pellet was resuspended in 100–200 µl Laemmli buffer containing 5–10 µl Tris base (1 M). The extracts were boiled for 5 min, centrifuged for 5 min at 12,000 rpm, and transferred to new tube. Protein concentration was determined by Bradford assay.

SDS-PAGE and Western blots
10–15 µg whole-cell extracts were run on 8–12% acryl–bisacrylamide (29:1) gels, except for Rad53 and Mad1 phosphorylation in which 15% SuperSep Phos-tag gels (Wako Chemicals USA) were used following the

manufacturer's instructions. Proteins were transferred to nitrocellulose membranes (Protran; Whatman) using wet blotting and revealed using standard immunoblotting and ECL procedures. Primary antibodies were rabbit polyclonal anti-DNA Pol-α B subunit (Pol12; 1:1,000; clone 6D2; gift from M. Foiani, Italian Foundation for Cancer Research Institute of Molecular Oncology, Milan, Italy), mouse monoclonal antimyc (1:1,000 from ascites for Pds1-18myc), mouse monoclonal anti-Rad53 (clone EL7; 1:20; obtained from M. Foiani), and rabbit polyclonal anti-Mad1 (1:3,000; obtained from K. Hardwick, Wellcome Trust, Edinburgh, Scotland, UK).

Online supplemental material
Fig. S1, related to Fig. 1, shows that DNA replication and anaphase are delayed in the conditional *GALS-CLB5 clb6* strain and that Rad53 is neither hyperphosphorylated during the delayed S phase nor required for the viability of *clb5,6* cells. Fig. S2 shows that Clb2 activation is delayed in vivo despite normal Clb2 protein accumulation (related to Fig. 2 A) and the FACS profiles for experiments reported in Fig. 3 B. Fig. S3 shows that bipolar spindles are made at similar times in wild-type and *clb5,6* cells (related to Fig. 1) and terminal phenotype of *clb5,6 mec1 mad2* cells (related to Fig. 3, A and D). Table S1 lists the yeast strains used in this study. Online supplemental material is available at http://www.jcb.org/cgi/content/full/jcb.201306023/DC1. Additional data are available in the JCB DataViewer at http://dx.doi.org/10.1083/jcb.201306023.dv.

References

Agarwal, R., and O. Cohen-Fix. 2002. Phosphorylation of the mitotic regulator Pds1/securin by Cdc28 is required for efficient nuclear localization of Esp1/separase. *Genes Dev.* 16:1371–1382. http://dx.doi.org/10.1101/gad.971402

Amon, A., U. Surana, I. Muroff, and K. Nasmyth. 1992. Regulation of p34CDC28 tyrosine phosphorylation is not required for entry into mitosis in *S. cerevisiae. Nature.* 355:368–371. http://dx.doi.org/10.1038/355368a0

Aparicio, O.M. 2013. Location, location, location: it's all in the timing for replication origins. *Genes Dev.* 27:117–128. http://dx.doi.org/10.1101/gad.209999.112

Bartek, J., and J. Lukas. 2007. DNA damage checkpoints: from initiation to recovery or adaptation. *Curr. Opin. Cell Biol.* 19:238–245. http://dx.doi.org/10.1016/j.ceb.2007.02.009

Brady, D.M., and K.G. Hardwick. 2000. Complex formation between Mad1p, Bub1p and Bub3p is crucial for spindle checkpoint function. *Curr. Biol.* 10:675–678. http://dx.doi.org/10.1016/S0960-9822(00)00515-7

Chen, R.H., J.C. Waters, E.D. Salmon, and A.W. Murray. 1996. Association of spindle assembly checkpoint component XMAD2 with unattached kinetochores. *Science.* 274:242–246. http://dx.doi.org/10.1126/science.274.5285.242

Cimprich, K.A., and D. Cortez. 2008. ATR: an essential regulator of genome integrity. *Nat. Rev. Mol. Cell Biol.* 9:616–627. http://dx.doi.org/10.1038/nrm2450

Cohen-Fix, O., and D. Koshland. 1997. The anaphase inhibitor of *Saccharomyces cerevisiae* Pds1p is a target of the DNA damage checkpoint pathway. *Proc. Natl. Acad. Sci. USA.* 94:14361–14366. http://dx.doi.org/10.1073/pnas.94.26.14361

Cohen-Fix, O., J.M. Peters, M.W. Kirschner, and D. Koshland. 1996. Anaphase initiation in *Saccharomyces cerevisiae* is controlled by the APC-dependent degradation of the anaphase inhibitor Pds1p. *Genes Dev.* 10:3081–3093. http://dx.doi.org/10.1101/gad.10.24.3081

Coudreuse, D., and P. Nurse. 2010. Driving the cell cycle with a minimal CDK control network. *Nature.* 468:1074–1079. http://dx.doi.org/10.1038/nature09543

Donaldson, A.D., M.K. Raghuraman, K.L. Friedman, F.R. Cross, B.J. Brewer, and W.L. Fangman. 1998. *CLB5*-dependent activation of late replication origins in *S. cerevisiae. Mol. Cell.* 2:173–182. http://dx.doi.org/10.1016/S1097-2765(00)80127-6

Dulev, S., C. de Renty, R. Mehta, I. Minkov, E. Schwob, and A. Strunnikov. 2009. Essential global role of *CDC14* in DNA synthesis revealed by chromosome underreplication unrecognized by checkpoints in *cdc14* mutants. *Proc. Natl. Acad. Sci. USA.* 106:14466–14471. http://dx.doi.org/10.1073/pnas.0900190106

Feng, W., J. Bachant, D. Collingwood, M.K. Raghuraman, and B.J. Brewer. 2009. Centromere replication timing determines different forms of genomic instability in *Saccharomyces cerevisiae* checkpoint mutants during replication stress. *Genetics.* 183:1249–1260. http://dx.doi.org/10.1534/genetics.109.107508

Foiani, M., G. Liberi, G. Lucchini, and P. Plevani. 1995. Cell cycle-dependent phosphorylation and dephosphorylation of the yeast DNA polymerase alpha-primase B subunit. *Mol. Cell. Biol.* 15:883–891.

Gietz, R.D., and A. Sugino. 1988. New yeast-*Escherichia coli* shuttle vectors constructed with in vitro mutagenized yeast genes lacking six-base pair restriction sites. *Gene.* 74:527–534. http://dx.doi.org/10.1016/0378-1119(88)90185-0

Gillett, E.S., C.W. Espelin, and P.K. Sorger. 2004. Spindle checkpoint proteins and chromosome–microtubule attachment in budding yeast. *J. Cell Biol.* 164:535–546. http://dx.doi.org/10.1083/jcb.200308100

Haber, J.E., H. Braberg, Q. Wu, R. Alexander, J. Haase, C. Ryan, Z. Lipkin-Moore, K.E. Franks-Skiba, T. Johnson, M. Shales, et al. 2013. Systematic triple-mutant analysis uncovers functional connectivity between pathways involved in chromosome regulation. *Cell Rep.* 3:2168–2178. http://dx.doi.org/10.1016/j.celrep.2013.05.007

Hardwick, K.G., and A.W. Murray. 1995. Mad1p, a phosphoprotein component of the spindle assembly checkpoint in budding yeast. *J. Cell Biol.* 131:709–720. http://dx.doi.org/10.1083/jcb.131.3.709

Hartwell, L.H., and T.A. Weinert. 1989. Checkpoints: controls that ensure the order of cell cycle events. *Science.* 246:629–634. http://dx.doi.org/10.1126/science.2683079

Hu, F., and O.M. Aparicio. 2005. Swe1 regulation and transcriptional control restrict the activity of mitotic cyclins toward replication proteins in *Saccharomyces cerevisiae. Proc. Natl. Acad. Sci. USA.* 102:8910–8915. http://dx.doi.org/10.1073/pnas.0406987102

Hyrien, O., and A. Goldar. 2010. Mathematical modelling of eukaryotic DNA replication. *Chromosome Res.* 18:147–161. http://dx.doi.org/10.1007/s10577-009-9092-4

Janke, C., M.M. Magiera, N. Rathfelder, C. Taxis, S. Reber, H. Maekawa, A. Moreno-Borchart, G. Doenges, E. Schwob, E. Schiebel, and M. Knop. 2004. A versatile toolbox for PCR-based tagging of yeast genes: new fluorescent proteins, more markers and promoter substitution cassettes. *Yeast.* 21:947–962. http://dx.doi.org/10.1002/yea.1142

Joglekar, A.P., K. Bloom, and E.D. Salmon. 2009. In vivo protein architecture of the eukaryotic kinetochore with nanometer scale accuracy. *Curr. Biol.* 19:694–699. http://dx.doi.org/10.1016/j.cub.2009.02.056

Kaiser, C., S. Michaelis, and A. Mitchell. 1994. Methods in Yeast Genetics: A Laboratory Course Manual. Cold Spring Harbor Laboratory Press, Cold Spring Harbor, NY. 202 pp.

Kelly, T.J., G.S. Martin, S.L. Forsburg, R.J. Stephen, A. Russo, and P. Nurse. 1993. The fission yeast *cdc18+* gene product couples S phase to START and mitosis. *Cell.* 74:371–382. http://dx.doi.org/10.1016/0092-8674(93)90427-R

Kinoshita, E., E. Kinoshita-Kikuta, K. Takiyama, and T. Koike. 2006. Phosphate-binding tag, a new tool to visualize phosphorylated proteins. *Mol. Cell. Proteomics.* 5:749–757. http://dx.doi.org/10.1074/mcp.T500024-MCP200

Kitamura, E., K. Tanaka, Y. Kitamura, and T.U. Tanaka. 2007. Kinetochore microtubule interaction during S phase in *Saccharomyces cerevisiae. Genes Dev.* 21:3319–3330. http://dx.doi.org/10.1101/gad.449407

Labib, K. 2010. How do Cdc7 and cyclin-dependent kinases trigger the initiation of chromosome replication in eukaryotic cells? *Genes Dev.* 24:1208–1219. http://dx.doi.org/10.1101/gad.1933010

Labib, K., S.E. Kearsey, and J.F. Diffley. 2001. MCM2-7 proteins are essential components of prereplicative complexes that accumulate cooperatively in the nucleus during G1-phase and are required to establish, but not maintain, the S-phase checkpoint. *Mol. Biol. Cell.* 12:3658–3667. http://dx.doi.org/10.1091/mbc.12.11.3658

Lengronne, A., and E. Schwob. 2002. The yeast CDK inhibitor Sic1 prevents genomic instability by promoting replication origin licensing in late G(1). *Mol. Cell.* 9:1067–1078. http://dx.doi.org/10.1016/S1097-2765(02)00513-0

Li, J.J., and R.J. Deshaies. 1993. Exercising self-restraint: discouraging illicit acts of S and M in eukaryotes. *Cell.* 74:223–226. http://dx.doi.org/10.1016/0092-8674(93)90413-K

Li, X., and R.B. Nicklas. 1995. Mitotic forces control a cell-cycle checkpoint. *Nature*. 373:630–632. http://dx.doi.org/10.1038/373630a0

Lisby, M., R. Rothstein, and U.H. Mortensen. 2001. Rad52 forms DNA repair and recombination centers during S phase. *Proc. Natl. Acad. Sci. USA*. 98:8276–8282. http://dx.doi.org/10.1073/pnas.121006298

Liu, H., and Y. Wang. 2006. The function and regulation of budding yeast Swe1 in response to interrupted DNA synthesis. *Mol. Biol. Cell*. 17:2746–2756. http://dx.doi.org/10.1091/mbc.E05-11-1093

Longtine, M.S., A. McKenzie III, D.J. Demarini, N.G. Shah, A. Wach, A. Brachat, P. Philippsen, and J.R. Pringle. 1998. Additional modules for versatile and economical PCR-based gene deletion and modification in *Saccharomyces cerevisiae*. *Yeast*. 14:953–961. http://dx.doi.org/10.1002/(SICI)1097-0061(199807)14:10<953::AID-YEA293>3.0.CO;2-U

Malumbres, M., and M. Barbacid. 2009. Cell cycle, CDKs and cancer: a changing paradigm. *Nat. Rev. Cancer*. 9:153–166. http://dx.doi.org/10.1038/nrc2602

McGuffee, S.R., D.J. Smith, and I. Whitehouse. 2013. Quantitative, genome-wide analysis of eukaryotic replication initiation and termination. *Mol. Cell*. 50:123–135. http://dx.doi.org/10.1016/j.molcel.2013.03.004

Michaelis, C., R. Ciosk, and K. Nasmyth. 1997. Cohesins: chromosomal proteins that prevent premature separation of sister chromatids. *Cell*. 91:35–45. http://dx.doi.org/10.1016/S0092-8674(01)80007-6

Miranda-Saavedra, D., M.J. Stark, J.C. Packer, C.P. Vivares, C. Doerig, and G.J. Barton. 2007. The complement of protein kinases of the microsporidium *Encephalitozoon cuniculi* in relation to those of *Saccharomyces cerevisiae* and *Schizosaccharomyces pombe*. *BMC Genomics*. 8:309. http://dx.doi.org/10.1186/1471-2164-8-309

Moore, J.D., J.A. Kirk, and T. Hunt. 2003. Unmasking the S-phase-promoting potential of cyclin B1. *Science*. 300:987–990. http://dx.doi.org/10.1126/science.1081418

Mumberg, D., R. Müller, and M. Funk. 1994. Regulatable promoters of *Saccharomyces cerevisiae*: comparison of transcriptional activity and their use for heterologous expression. *Nucleic Acids Res*. 22:5767–5768. http://dx.doi.org/10.1093/nar/22.25.5767

Murga, M., S. Bunting, M.F. Montaña, R. Soria, F. Mulero, M. Cañamero, Y. Lee, P.J. McKinnon, A. Nussenzweig, and O. Fernandez-Capetillo. 2009. A mouse model of ATR-Seckel shows embryonic replicative stress and accelerated aging. *Nat. Genet*. 41:891–898. http://dx.doi.org/10.1038/ng.420

Nasmyth, K. 1996. At the heart of the budding yeast cell cycle. *Trends Genet*. 12:405–412. http://dx.doi.org/10.1016/0168-9525(96)10041-X

Petermann, E., A. Maya-Mendoza, G. Zachos, D.A. Gillespie, D.A. Jackson, and K.W. Caldecott. 2006. Chk1 requirement for high global rates of replication fork progression during normal vertebrate S phase. *Mol. Cell. Biol*. 26:3319–3326. http://dx.doi.org/10.1128/MCB.26.8.3319-3326.2006

Piatti, S., C. Lengauer, and K. Nasmyth. 1995. Cdc6 is an unstable protein whose de novo synthesis in G1 is important for the onset of S phase and for preventing a 'reductional' anaphase in the budding yeast *Saccharomyces cerevisiae*. *EMBO J*. 14:3788–3799.

Raghuraman, M.K., E.A. Winzeler, D. Collingwood, S. Hunt, L. Wodicka, A. Conway, D.J. Lockhart, R.W. Davis, B.J. Brewer, and W.L. Fangman. 2001. Replication dynamics of the yeast genome. *Science*. 294:115–121. http://dx.doi.org/10.1126/science.294.5540.115

Rhind, N., S.C. Yang, and J. Bechhoefer. 2010. Reconciling stochastic origin firing with defined replication timing. *Chromosome Res*. 18:35–43. http://dx.doi.org/10.1007/s10577-009-9093-3

Schwob, E., T. Böhm, M.D. Mendenhall, and K. Nasmyth. 1994. The B-type cyclin kinase inhibitor p40SIC1 controls the G1 to S transition in *S. cerevisiae*. *Cell*. 79:233–244. http://dx.doi.org/10.1016/0092-8674(94)90193-7

Shiotani, B., and L. Zou. 2009. Single-stranded DNA orchestrates an ATM-to-ATR switch at DNA breaks. *Mol. Cell*. 33:547–558. http://dx.doi.org/10.1016/j.molcel.2009.01.024

Sørensen, C.S., R.G. Syljuåsen, J. Lukas, and J. Bartek. 2004. ATR, Claspin and the Rad9-Rad1-Hus1 complex regulate Chk1 and Cdc25A in the absence of DNA damage. *Cell Cycle*. 3:941–945. http://dx.doi.org/10.4161/cc.3.7.972

Sorger, P.K., and A.W. Murray. 1992. S-phase feedback control in budding yeast independent of tyrosine phosphorylation of p34cdc28. *Nature*. 355:365–368. http://dx.doi.org/10.1038/355365a0

Tanaka, S., and H. Araki. 2010. Regulation of the initiation step of DNA replication by cyclin-dependent kinases. *Chromosoma*. 119:565–574. http://dx.doi.org/10.1007/s00412-010-0291-8

Tercero, J.A., M.P. Longhese, and J.F. Diffley. 2003. A central role for DNA replication forks in checkpoint activation and response. *Mol. Cell*. 11:1323–1336. http://dx.doi.org/10.1016/S1097-2765(03)00169-2

Torres-Rosell, J., G. De Piccoli, V. Cordon-Preciado, S. Farmer, A. Jarmuz, F. Machin, P. Pasero, M. Lisby, J.E. Haber, and L. Aragón. 2007. Anaphase onset before complete DNA replication with intact checkpoint responses. *Science*. 315:1411–1415. http://dx.doi.org/10.1126/science.1134025

Van, C., S. Yan, W.M. Michael, S. Waga, and K.A. Cimprich. 2010. Continued primer synthesis at stalled replication forks contributes to checkpoint activation. *J. Cell Biol*. 189:233–246. http://dx.doi.org/10.1083/jcb.200909105

Weinert, T.A., and L.H. Hartwell. 1988. The *RAD9* gene controls the cell cycle response to DNA damage in *Saccharomyces cerevisiae*. *Science*. 241:317–322. http://dx.doi.org/10.1126/science.3291120

Zegerman, P., and J.F. Diffley. 2010. Checkpoint-dependent inhibition of DNA replication initiation by Sld3 and Dbf4 phosphorylation. *Nature*. 467:474–478. http://dx.doi.org/10.1038/nature09373

Zou, L., and S.J. Elledge. 2003. Sensing DNA damage through ATRIP recognition of RPA-ssDNA complexes. *Science*. 300:1542–1548. http://dx.doi.org/10.1126/science.1083430